

PROJECT REPORT (Final)

Project ID/Title: **Investigation of the effects of various defects in metallic specimens on the spatial distribution of pulsed eddy currents**

Project Sponsor: MOHE

Project ID: FRGS16-059-0558

Author Name(s): Dr. Ali Sophian , Faris Nafiah

Department/Kulliyah/Institute/Centre: Mechatronics/Engineering

Abstract

Intro on PEC,

Pulsed eddy current (PEC) NDT&E has been around for some time and it is still attracting extensive attention from researchers around the globe. Thanks to its richness of spectral components, various applications of this technique have been proposed and reported in the literature covering both structural integrity inspection and material characterization in various industrial sectors. In this project it was hypothesized that the spatial and temporal magnetic field signals can offer more information of the defects compared to single point data, which have been proven in this project, through numerical modelling and analysis of experimental data gathered by using a PEC system developed in the project. In this project, it has been shown that there is some unique correlation between the spatial distribution of the eddy current and the characteristics of defects, including their sizes. In this project, particularly this was studied by using normal and inclined cracks that are located on both surface and sub-surface. This finding can be utilized to enrich even further the information that we can extract from PEC signals.

Introduction^[as1]

Pulsed eddy current (PEC) NDT&E has been around for some time and it is still attracting extensive attention from researchers around the globe, which can be witnessed through the reports reviewed in this paper. Thanks to its richness of spectral components, various applications of this technique have been proposed and reported in the literature covering both structural integrity inspection and material characterization in various industrial sectors.

The state-of-the-art research in sensors exploits the use of multiple sensors or array of sensors. In PEC NDT, this can potentially be offering even more information to be extracted. Because of this potential, the investigation on the use of PEC signal map for characterizing defects was conducted in this project. An array of sensors could produce a 2D map of representation of the PEC magnetic field signal, which is also known as a C-scan in NDT. In this research, due to limited access to arrayed magnetic sensors, the distribution map was generated through scanning of the probe.

This report presents the work that has been carried out in a MOHE-funded FRGS project.

Background

With the rapid growth of urban development and transportation technology, increasing demands for a better inspection system on steel structures must be fulfilled. Failure in doing so would most likely deliver serious drawbacks.

Pulsed eddy current (PEC) technique is used for the detection and characterization of both surface and sub-surface defects in metallic objects. The defects include cracks and corrosion or wall thinning. Presently, the information regarding the defect that can be obtained by using PEC is still limited. In order to extend the application of PEC techniques, the reliability and richness of information needs to be enhanced. The reliability of PEC is affected by the variation in the lift-off. If the defect's characteristics can be inferred by using the spatial distribution of the transient magnetic field, PEC technique may offer richer information within a relatively shorter time, which will bring more benefits for many NDT applications.

Objectives

1. To build FE models for pulsed eddy current excitation coils and samples
2. To investigate the correlation between the spatial distribution of pulsed eddy currents and the defect's characteristics.
3. To evaluate the use of the correlation in characterization of artificial defects by experimental tests

Methodology

The research was conducted through both model-based investigation and empirical tests.

A number of finite element models of excitation coils and samples were developed by using COMSOL, both 2D and 3D.

For each test condition, the distribution of the eddy current and its induced magnetic field was studied, both spatially and temporally. As for the magnetic field, the differential magnetic field strength, especially its time to peak and peak value, was used in the analysis.

An experimental setup was designed and implemented, which included excitation coils, 2-axis scanning system, excitation system and data acquisition (DAQ) system. In this experiment, the scanning mechanism was used to capture the distribution or mapping of the magnetic field on the surface of the sample. Samples with selected artificial defects (both surface and sub-surface) of different types and sizes were designed, manufactured and, then, used during this experiment. Data obtained from the experiments was used to validate and evaluate the findings obtained from the model-based investigation.

The acquired signals were then post-processed to construct C-scan images for all the cracks. Through this, the information regarding the spatial distribution of magnetic field across the tested samples was evaluated. Consequently, feature extraction strategy was devised from the C-scan image, with the prerequisite of the knowledge obtained from the numerical modelling

Novel image-based features were proposed, which was capable of distinguishing crack classes, as well as quantifying the inclined surface crack parameters. Besides, this stage also provided the insight into the reliability of the feature through feature analysis. Three regression models were built to propose a technique in handling the interdependency posed by the features.

Results

Modelling

A number of finite element models of excitation coils and samples were developed by using COMSOL, both 2D and 3D. Figure 1 shows one of the models that was developed for studying inclined cracks.

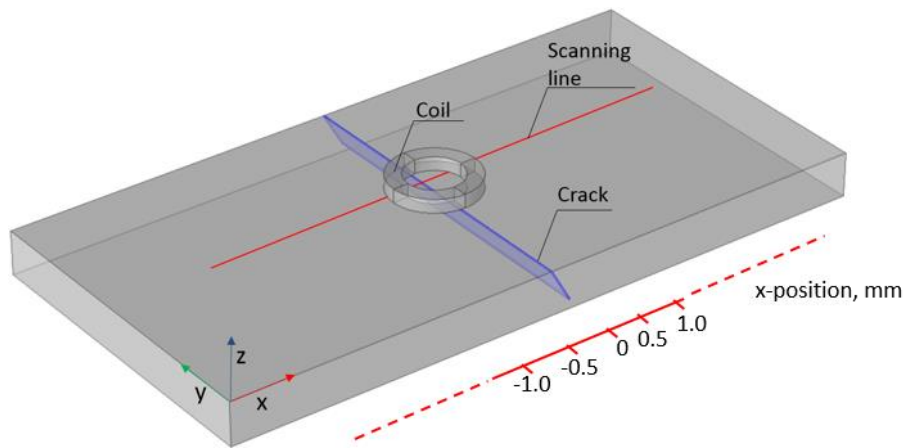


Figure 1 Geometry of the constructed FEM using COMSOL Multiphysics. Crack was configured as a geometry itself, instead of a slot elongating across the test piece width.

For accuracy and speed optimisation, it was found that the model stopped converging at 'Finer' mesh configuration with a deviation of 0.44% from the axisymmetric model, as seen in Figure 2. The results from mesh convergence analysis served to provide mesh configuration options to the consequent analysis.

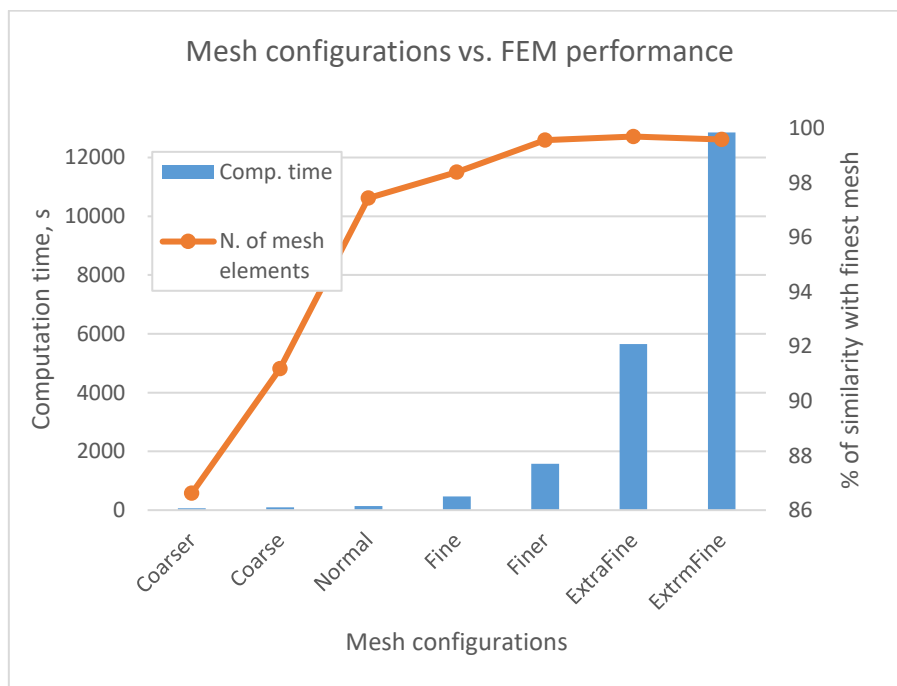
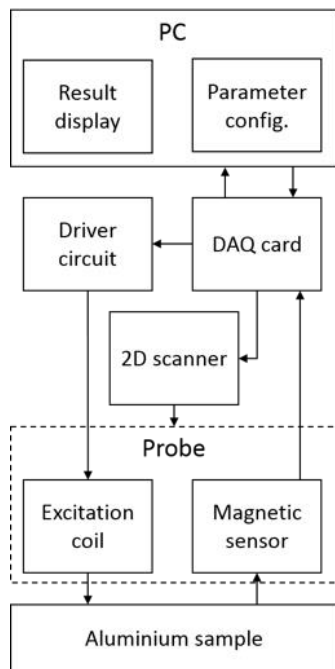


Figure 2 Mesh convergence analysis

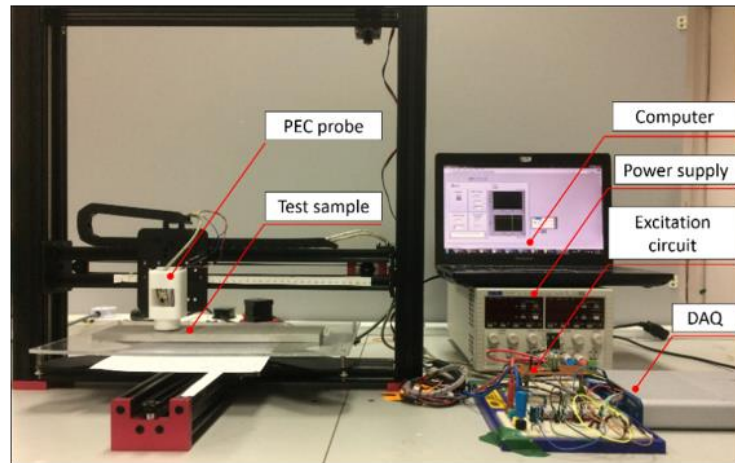
PEC System Design

To anticipate the necessity of this work, the development of the PEC system was customised to have a system design as shown in Figure 3. Briefly, the flow of the system worked as follows: the user specified the excitation and scanning parameters. The DAQ card executed the specified tasks from the computer (PC) and supplied the driver circuit with current waveform signals. The driver circuit amplified the waveform signal to the specified current value to be fed to the excitation coil. The magnetic sensor, placed in the middle of the coil, acquired the resultant magnetic flux density to be

stored in the PC via the DAQ card. The PC pre-processed the information to display the differential signal, the peak value and the peak arrival time. Subsequently, the probe was moved by the 2D scanner by the specified resolution. The process was repeated for each spatial resolution until the scanning area specified by the user was covered.



(a)



(b)

Figure 3 (a) The block diagram of the overall PEC system design, and (b) experimental setup

Figure 4 shows the probe design and its holder.

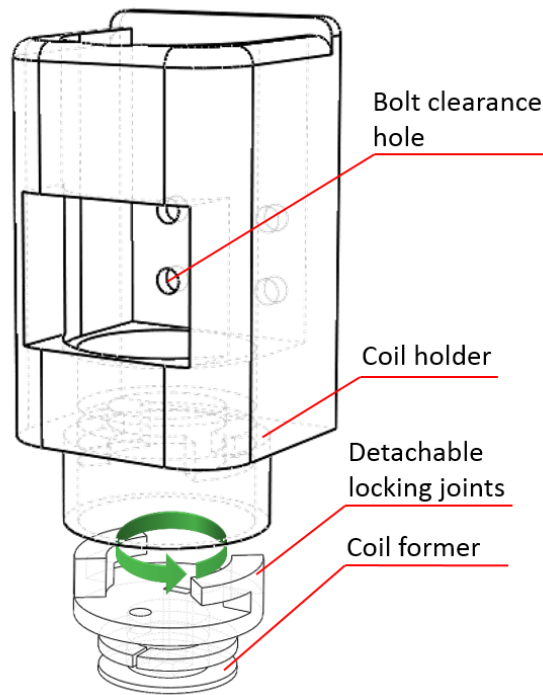
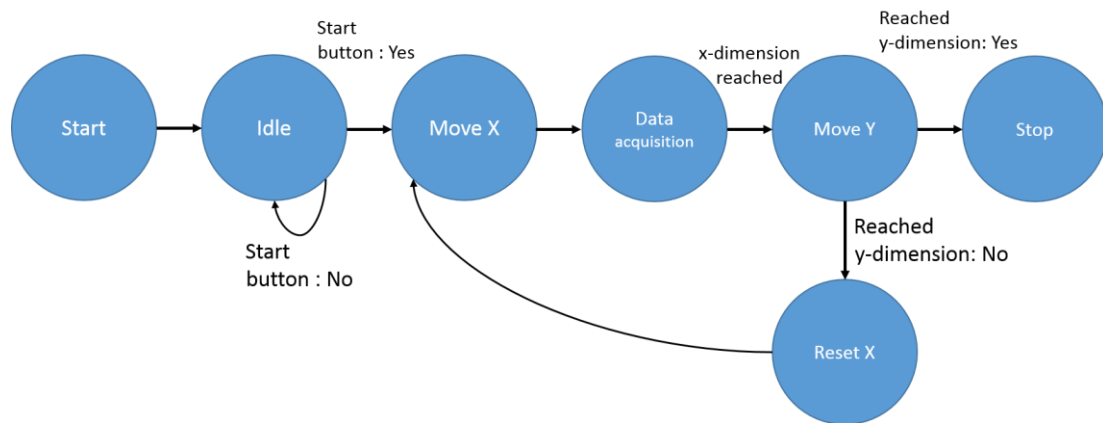


Figure 4 (Geometrical design of the coil former and the coil holder)

Figure 5 illustrates how the software and hardware of the system works in gathering scanning data.



(a)

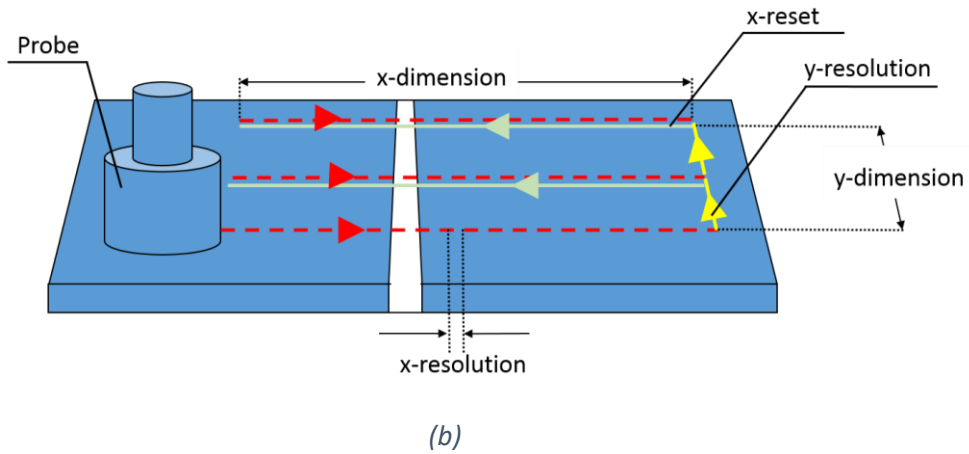


Figure 5 (a) The state machine of the LabVIEW graphical codes and (b) illustration of the scanning flow

Manufactures Samples

For the experiment, samples of defects had to be made. The following tables show the defects that were established and used the project.

Table1 Surface crack parameters

Surface crack parameters		
Crack inclination angle (°)	Crack depth (mm)	Width (mm)
30±0.5	(2, 4, 6, 8) ±0.2	0.35 ±0.05
45±0.5	(2, 4, 6, 8) ±0.2	0.35 ±0.05
60±0.5	(2, 4, 6, 8) ±0.2	0.35 ±0.05
75±0.5	(2, 4, 6, 8) ±0.2	0.35 ±0.05
90±0.5	(2, 4, 6, 8) ±0.2	0.35 ±0.05

Table2 Subsurface crack parameters

Surface crack parameters		
Crack inclination angle (°)	Crack depth (mm)	Width (mm)
30±0.5	2 ±0.2	0.35 ±0.05
45±0.5	2 ±0.2	0.35 ±0.05
60±0.5	2 ±0.2	0.35 ±0.05
75±0.5	2 ±0.2	0.35 ±0.05
90±0.5	2 ±0.2	0.35 ±0.05

Table3 Blind test crack parameters

Blind test crack parameters		
Crack inclination angle (°)	Crack depth (mm)	Width (mm)
32±0.5	5 ±0.2	0.35 ±0.05
50±0.5	6 ±0.2	0.35 ±0.05
75±0.5	5 ±0.2	0.35 ±0.05

Data Gathering

By using the developed PEC system, data were gathered by using samples of various cracks. Figure 6 illustrates a sample of C-scan data from an inclined crack sample.

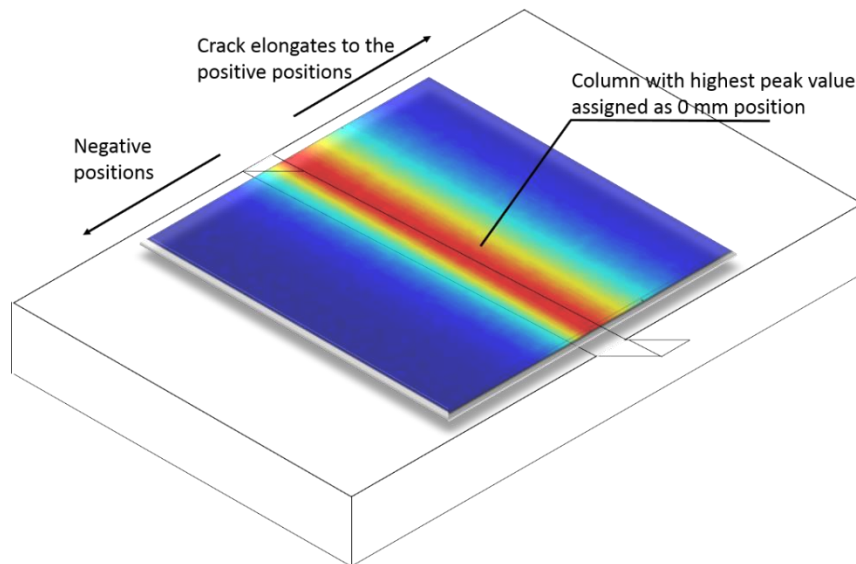


Figure 6 Spatial positioning based on the highest peak value in one of the rows of the image

Figure 7 show C-scan images generated by using different signal features, both time and frequency domains.

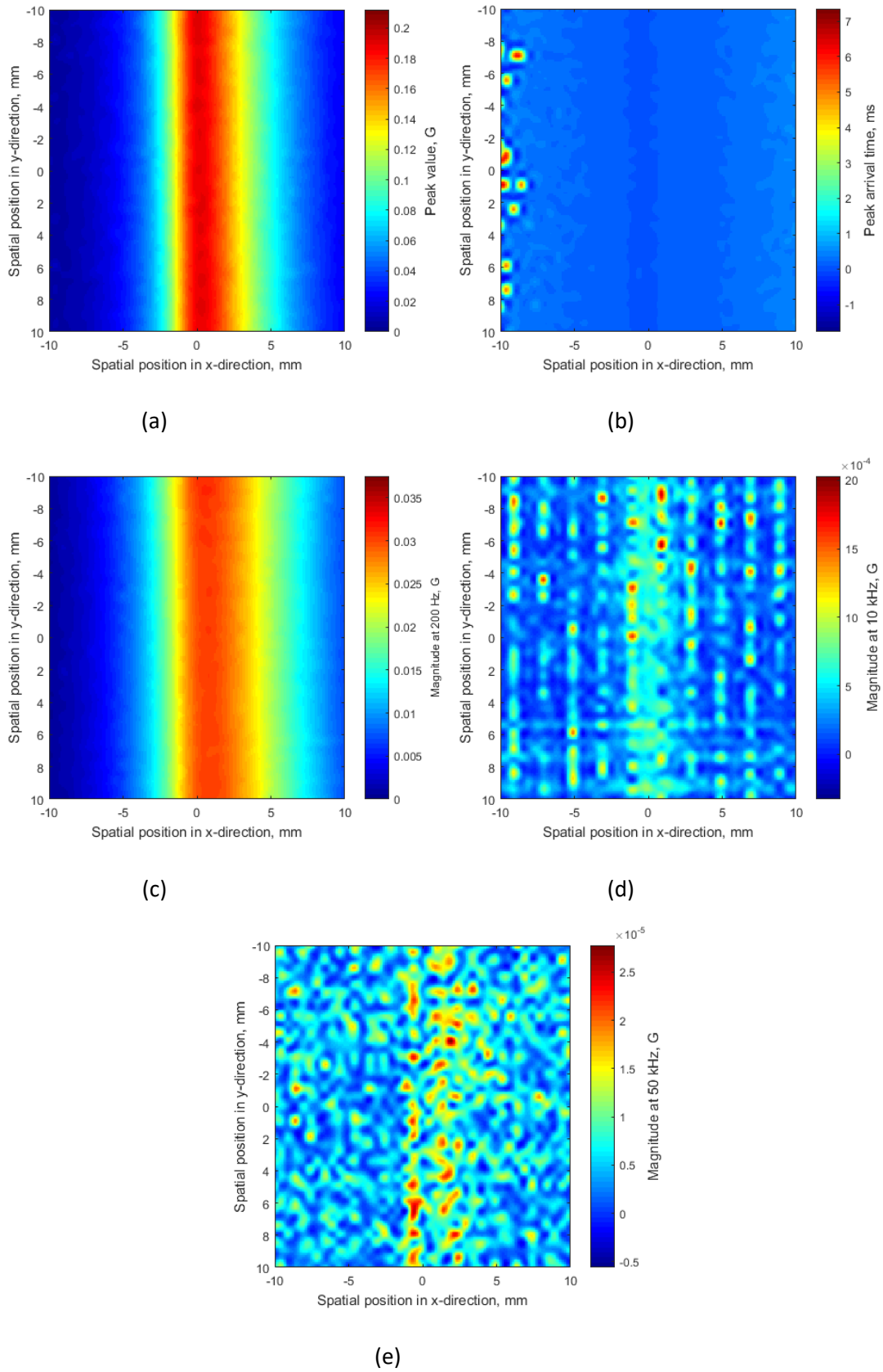


Figure 7 C-scan images constructed using (a) peak value, (b) peak arrival time, (c) magnitude at 200 Hz, (d) magnitude at 10 kHz, (e) magnitude at 50 kHz

Data Analysis

For the study case, some inclined cracks are studied here. Figure 8 visualises the magnetic flux density in z-direction (into the plane) as well as the induced eddy current, for a flawless test piece and a test piece with a crack respectively. As observed, the magnetic field (denoted with magnetic flux density) beneath the inner region of the coil exhibited a circular form for a flawless test piece, indicating that the region near the coil contained the highest magnitude of magnetic field, while it deteriorated with the distance away from the coil. Compared to a flawless test piece, the test piece with 90° crack exhibited a concentration of higher magnitude of magnetic field in the region near the crack. This can be inferred with the decline of the induced eddy current (white arrow) in the region, which consequently reduced the magnitude of the secondary magnetic field opposing the injected magnetic field. Besides, the crack interrupted the flow of the induced eddy current, which resulted in a fluctuation of magnetic flux density in the region near the crack. This can be explained with the depth of penetration formula, where the crack face was also treated as a conductor surface by the eddy current.

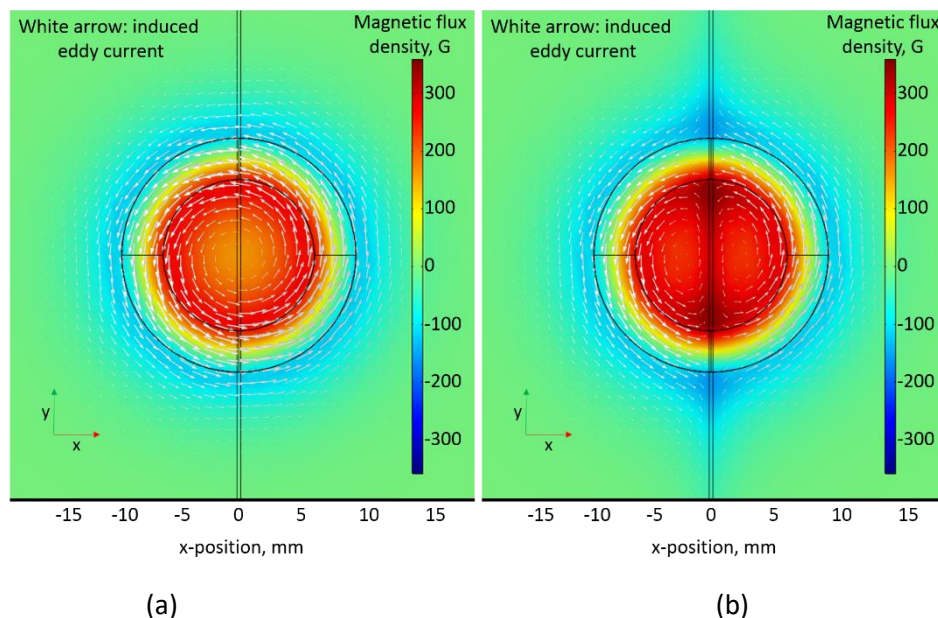


Figure 8 Top view of magnetic flux density for (a) flawless sample and (b) sample with 90° crack

Figure 9 (a)-(f) further prove the skin depth formula, as mentioned in the above justification as well as in the literature review in Chapter 2. The side view gives a detailed information on the decline of the magnetic flux density with depth. In addition, it can also be observed that the magnetic flux density intensified at the edges, i.e. crack faces and tested sample surfaces, demonstrating the higher concentration of induced eddy current at shallower depths. Moving the coil to 3.5 mm away from the crack opening to either side of the crack face showed a similar response of the magnetic flux density and eddy current concentration (only the effect was inverted) for 90° crack. While that is true, the interaction of the PEC system to the 60° crack was different at spatial position of -3.5 mm and 3.5 mm, giving different form of magnetic field intensity. The concentration of the induced eddy current, as looked at the point beneath the middle of the coil for Figure 3.5 (e) and (f), were in contrast with each other. At position of -3.5 mm, the magnetic flux density was hugely dependent on its interaction with the eddy current near the test piece surface. Meanwhile, at 3.5 mm, the magnetic flux density can be

seen to interact with the eddy current near the test piece surface as well as the crack face due to the elongation of the crack towards the positive spatial positions. This was expected to give a different response signals to the magnetic sensor during experiment, benefitting the study by providing one of the potential features in discriminating crack inclination angles.

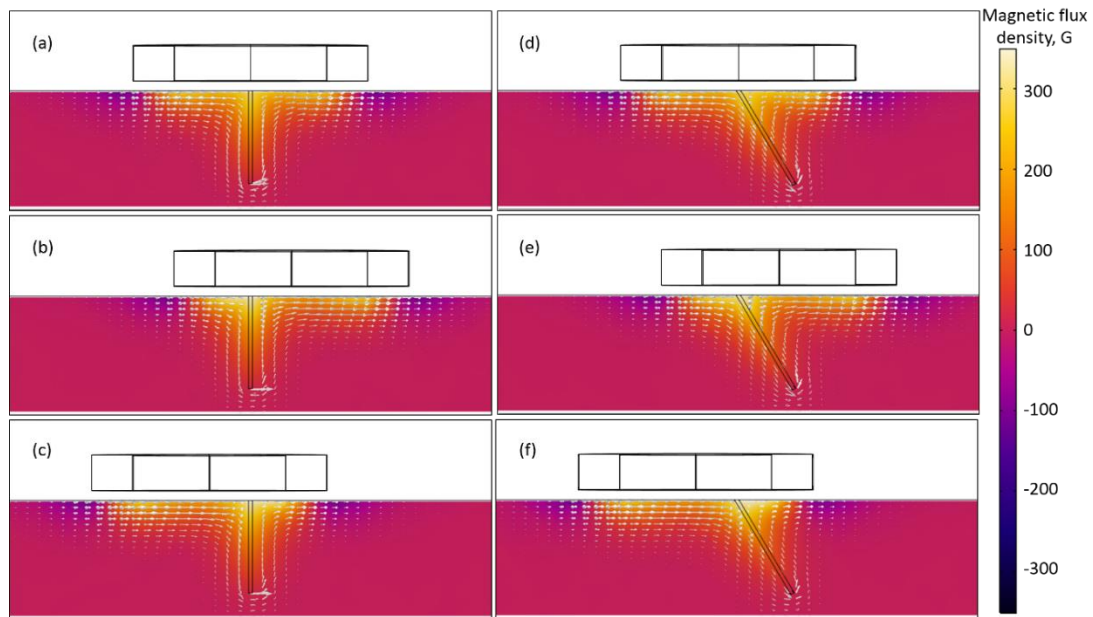
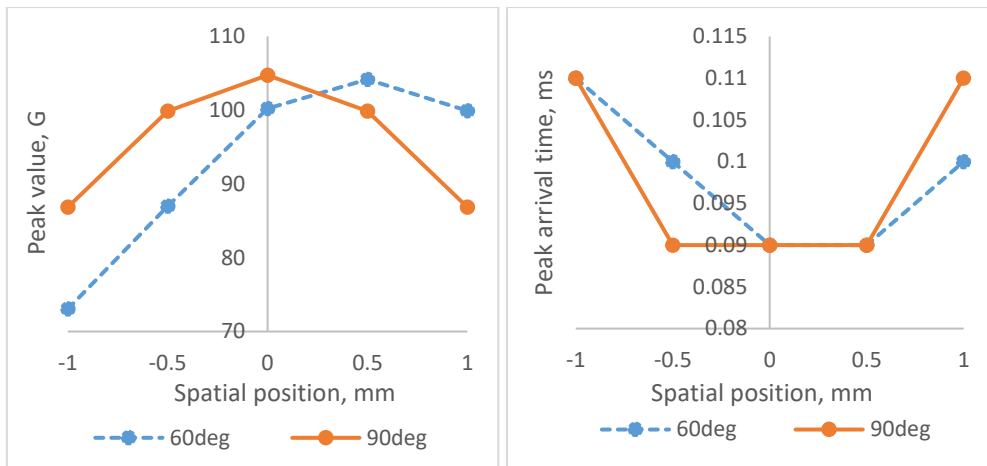


Figure 9 Magnetic field distribution of crack of (a) 90° at 0 mm, (b) 90° at 3.5 mm, (c) 90° at -3.5 mm, (d) 60° at 0 mm, (e) 60° at 3.5 mm and (f) 60° at -3.5 mm

The extracted peak value and peak arrival time in 5 (a) and (b) show a better visualisation of the effect of the crack on the spatial positions. Surprisingly, the signal with the highest amplitude for 60° crack was observed to be at the spatial position of 0.5 mm, unlike 90° crack which was at the middle of the crack opening. This can be explained with the concentration of the eddy current near the crack edges. Crack of 90° intensified the eddy current near the crack face only. Meanwhile, for 60° crack, at 0.5 mm spatial position, the induced eddy current was observed to be concentrated in the region near the crack face as well as the sample surface. This strengthened the secondary magnetic field even more, particularly at that position. However, the peak value at 1 mm was disappointed by the hypothesis as the eddy current was too deep, which consequently weakened the induced secondary magnetic field.

Although the peak arrival time was complicated to be differentiated between each position due to the low sampling resolution, the graph in Figure 10(b) still clearly shows the effects of cracks on the distribution of magnetic field. As for the 60° crack, the growth of the crack to the positive positions results in a right-skewed trend of the peak arrival time. Noting that peak arrival time explained the depth information (Krause et al., 2003), the positive positions demonstrated lower peak arrival time than the corresponding negative positions.

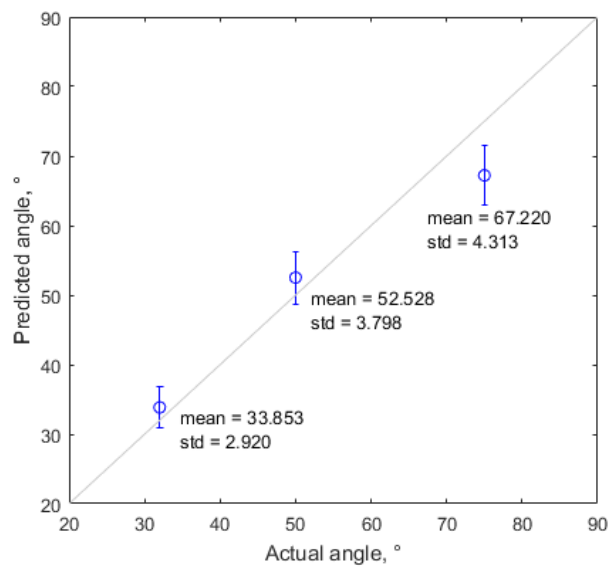


(a)

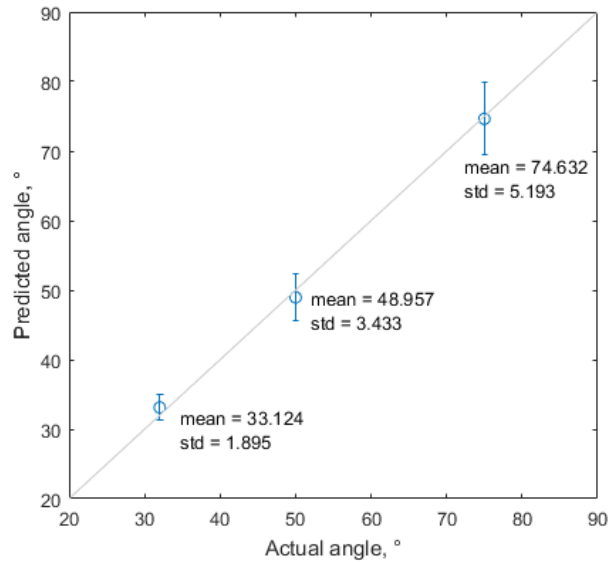
(b)

Figure 10 Extracted (a) peak value and (b) peak arrival time from differential signals at different spatial positions for 90° and 60° crack

Figure 11 shows the result of defect quantification by using the spatial distribution of the PEC signal, which shows that quantification is achievable by using this approach compared to single-point data.



(a)



(b)

Figure 11 Comparisons of fitting line and fitting model results in inclination angle prediction, for (a) HLM and (b) ANN

Findings

- The 2D axisymmetric model has been validated by the experimental results with an average error of less than 10%, indicating that it is a useful and reliable tool for predicting the performance of a PEC probe design in sample thickness measurement.
- The larger the diameter of the excitation coil, the deeper the penetration. However, although the larger diameters have deeper penetration, the smallest diameter has the highest sensitivity if normalization is not used. With all these conclusions, coil diameter plays a significant role in the optimization of a probe design and has to be taken into careful consideration.
- Image-based feature extraction strategy: The proposition of employing image processing in feature extraction is novel in PEC C-scan image analysis, where most of the previous research simply drew out linear scan responses from constructed C-scan images by drawing out a line of pixel values from the images. This is impractical in real life situations, where scanning of PEC probe may not be exceptionally perpendicular to the crack axis. The image processing technique suggested the localisation of the crack axis first, before drawing out pixel values orthogonal to the detected crack axis.
- Surface crack inclination angle quantifications: This research opened up the utilisation of PEC in quantifying crack inclination angles, despite the depths, among others. Three image-based features were proposed, the LLS, the skewness, and the LSmax, which were proven to offer linear dependencies with both inclination angles and depths.

Conclusions

The objectives of the project have been achieved. It has shown that there is some unique correlation between the spatial distribution of the eddy current and the characteristics of defects, including their sizes. In this project, particularly this was studied by using normal and inclined cracks that are located

on both surface and sub-surface. This finding can be utilized to enrich even further the information that we can extract from PEC signals. The outcome of the project, including the setup of the PEC measurement system can be utilized for further research projects.

Output

1. A set-up for conducting the experiment
2. Collection of PEC signal data
3. 2 published **scopus**-indexed journal publications
 - a. Pulsed eddy current non-destructive testing and evaluation: A review, Ali Sophian, Guiyun Tian, Mengbao Fan, 2017/5, Chinese Journal of Mechanical Engineering
 - b. Pulsed Eddy Current Imaging of Inclined Surface Cracks, Faris Nafiah, Ali Sophian, 2017/12/1, Indonesian Journal of Electrical Engineering and Informatics (IJEEI)
4. 2 in-review **scopus**-indexed journal publications
 - a. Modelling of Scanning Pulsed Eddy Current Testing of Normal and Slanted Surface Cracks
 - b. Image-based Feature Extraction Technique for Inclined Crack Quantification
5. 1 International conference publication
 - a. Modelling of Scanning Pulsed Eddy Current Testing of Normal and Slanted Surface Cracks, ESEM 2017, France
 - b. Effects of coil diameter in thickness measurement using pulsed eddy current non-destructive testing , IOP Conference Series: Materials Science and Engineering 260 (1) (**Scopus**-indexed)
6. 1 Full-research Mode MSc student (completed)
 - a. Thesis: PULSED EDDY CURRENT NDT FOR QUANTITATIVE EVALUATION OF INCLINED CRACKS

Future Plan of the research

- To investigate more specific applications, such as inspection of corrosion in pipes
- To build a portable prototype of the PEC NDT system

References

Please refer to the published paper and thesis for references used in this project.